



Cite this: *Lab Chip*, 2022, 22, 4792

Inertial microfluidics: current status, challenges, and future opportunities

Nan Xiang * and Zhonghua Ni

Inertial microfluidics uses the hydrodynamic effects induced at finite Reynolds numbers to achieve passive manipulation of particles, cells, or fluids and offers the advantages of high-throughput processing, simple channel geometry, and label-free and external field-free operation. Since its proposal in 2007, inertial microfluidics has attracted increasing interest and is currently widely employed as an important sample preparation protocol for single-cell detection and analysis. Although great success has been achieved in the inertial microfluidics field, its performance and outcome can be further improved. From this perspective, herein, we reviewed the current status, challenges, and opportunities of inertial microfluidics concerning the underlying physical mechanisms, available simulation tools, channel innovation, multistage, multiplexing, or multifunction integration, rapid prototyping, and commercial instrument development. With an improved understanding of the physical mechanisms and the development of novel channels, integration strategies, and commercial instruments, improved inertial microfluidic platforms may represent a new foundation for advancing biomedical research and disease diagnosis.

Received 2nd August 2022,
Accepted 30th September 2022

DOI: 10.1039/d2lc00722c

rsc.li/loc

Introduction

Inertial microfluidics takes advantage of the inherent inertial effects of microfluids at finite Reynolds numbers to passively

manipulate particles, cells, or fluids in a high-throughput and label-free manner.¹ Compared to active manipulation techniques based on external factors (such as electric,² magnetic,³ acoustic,⁴ and optical⁵ fields), inertial microfluidics allows high throughput processing, a simple channel geometry for easy fabrication, and passive and external field-free operation. Although research on inertial effects in macroscopic flows dates back to 1960s⁶ or even earlier,⁷ the concept of inertial microfluidics was first proposed in 2007.⁸

School of Mechanical Engineering, and Jiangsu Key Laboratory for Design and Manufacture of Micro-Nano Biomedical Instruments, Southeast University, Nanjing, 211189, China. E-mail: nan.xiang@seu.edu.cn



Nan Xiang

University in 2014. His research interests include inertial microfluidics, soft robotics, microfluidic cell separation and detection, and point-of-care testing devices.

Nan Xiang is a Professor in the School of Mechanical Engineering at Southeast University, Nanjing, China. He is now the PI of the Microfluidics and Soft Robotics Group at the Jiangsu Key Laboratory for Design and Manufacture of Micro-Nano Biomedical Instruments. He received his B.E. degree in Biosystems Engineering from Zhejiang University in 2009 and his Ph.D. degree in Mechanical Engineering from Southeast



Zhonghua Ni

microdevices, and biosensors.

Zhonghua Ni is a Professor in the School of Mechanical Engineering and the director of the Jiangsu Key Laboratory for Design and Manufacture of Micro-Nano Biomedical Instruments, Southeast University, Nanjing, China. He received his B.E. degree from the China University of Petroleum in 1990 and his Ph.D. degree from Southeast University in 2001. His research interests include microfluidics, biomedical

Over the past 15 years, inertial microfluidics has attracted increasing interest and has been widely employed for the rapid mixing of different specimens,⁹ efficient focusing,¹⁰ trapping,¹¹ and sorting¹² of cells, and for engineering fluid interfaces.^{13,14} These sample pretreatment functions play an important role in sheathless flow cytometric counting, label-free cell mechanical phenotyping, electrical impedance characterization, and cellular image analysis, among other protocols.^{15,16} For example, inertial focusing enables cells to pass through the detection region one by one at fixed positions, which significantly reduces detection errors caused by variations in the cell position and the presence of multiplex cells in the detection region.^{10,17,18} Cell separation is another important function of inertial microfluidic devices; based on the differential focusing positions and statuses, high-throughput and label-free cell separation can be achieved based on differences in cell size, shape, and deformability.^{19–21} Inertial cell separation has become an important pretreatment method for the detection and assessment of rare cell populations in large-volume complex samples.

To realize efficient cell manipulation, diverse channel geometries including spiral, straight, serpentine, and contraction–expansion channels have been designed.²² In addition, various new channel designs with modified planar geometries and nonrectangular cross-sections have been developed to achieve new manipulation functions and improved performance. The bending of channel patterns and the addition of design elements (such as expansion cavities and micropillars) make particle migration physics more complex.^{22–24} To date, many efforts have been made to uncover the physics behind the phenomena and discover new mechanisms for guiding and understanding the design of devices through experimental and numerical approaches. In addition to channel innovations, multistage, multiplexing, or multifunction integration of inertial microfluidics has been performed to achieve enhanced performance. The fundamentals,^{1,25,26} computation,²⁷ channel design,²² and novel applications²⁸ of inertial microfluidics are reviewed elsewhere. The readers could also refer to some excellent early comprehensive reviews.^{10,24,29} Although great success has been achieved in the field of inertial microfluidics, an improved understanding of the underlying physical mechanisms and the development of novel channels, integration strategies, and commercial instruments are still needed for diversified applications.

Herein, instead of providing a comprehensive review, we present the current status, challenges, and future opportunities of inertial microfluidics. In contrast to previous critical reviews, we focused on the aspects of physical mechanisms, simulation tools, channel innovation, multistage, multiplexing, or multifunction integration, rapid prototyping, and commercial instruments. First, we introduce the physical mechanisms and simulation tools available for guiding device design, and we summarize the most recent advances in channel innovation and multi-stage,

multiplexing, or multi-function integration for improved performance or new functions. Finally, advances in rapid prototyping techniques for the fabrication of novel inertial microfluidics and development of commercial instruments based on inertial microfluidics are presented.

New physical mechanisms and simulation tools for guiding device design

Various nonlinear flow phenomena are involved in inertial microfluidics (Fig. 1). For example, inertial migration induced by the inertia of microfluids at finite Reynolds numbers causes lateral particle migration perpendicular to the main flow streams, focusing the particles toward specific equilibrium positions in the cross section.^{10,30} Furthermore, new channels with increased curvature and sudden expansion can induce additional flow phenomena of cross-sectional Dean flow and planar vortexes, which modify the equilibrium positions and accelerate the particle migration process.^{1,22,24} The viscoelasticity effect, shear thinning, shear thickening, and other viscoelastic instability effects will also affect particle migration in most biological non-Newtonian or viscoelastic fluids prepared by adding an artificial elasticity enhancer of macromolecular polymers.^{31–34} Hence, coupling these nonlinear flow phenomena in inertial microfluidics makes it difficult to predict the particle migration process accurately.

Although several studies have explored the separate flow phenomenon in macroscopic flows, the understanding of these coupled flow phenomena in microscale inertial flows remains unclear. Recently, researchers have made great efforts to improve the understanding of particle migration in inertial microfluidics. Representative studies include the particle focusing process along the channel,^{18,35} effects of critical channel structures,³⁶ flow rate,^{37–39} and fluid properties^{8,38} on particle focusing in various channels, modified force scaling of inertial lift force,^{40–42} formation mechanisms of Dean flow,^{43,44} and particle–particle interactions in the focused particle train.⁴⁵ Although great success has been achieved over the past few decades, there is still room for improvement. First, systematic design rules are lacking. Currently, device design is mostly based on experimental trials and errors. Moreover, the universality of most experimental observations and existing design rules is poor, making the use of these findings or rules confined to one device. Therefore, establishing universal design rules for a specific type of channel will support the wide propagation of inertial microfluidics. Second, the interpretation of most new experimental observations still relies on speculation of possible mechanisms. The scaling of forces in inertial flows, such as inertial lift (F_L which is the net lift force of a shear-induced inertial lift force (F_{LS}) and a wall-induced inertial lift force (F_{LW})), Dean drag (F_D), and elastic forces (F_E), still depends on those obtained from studies on simplified

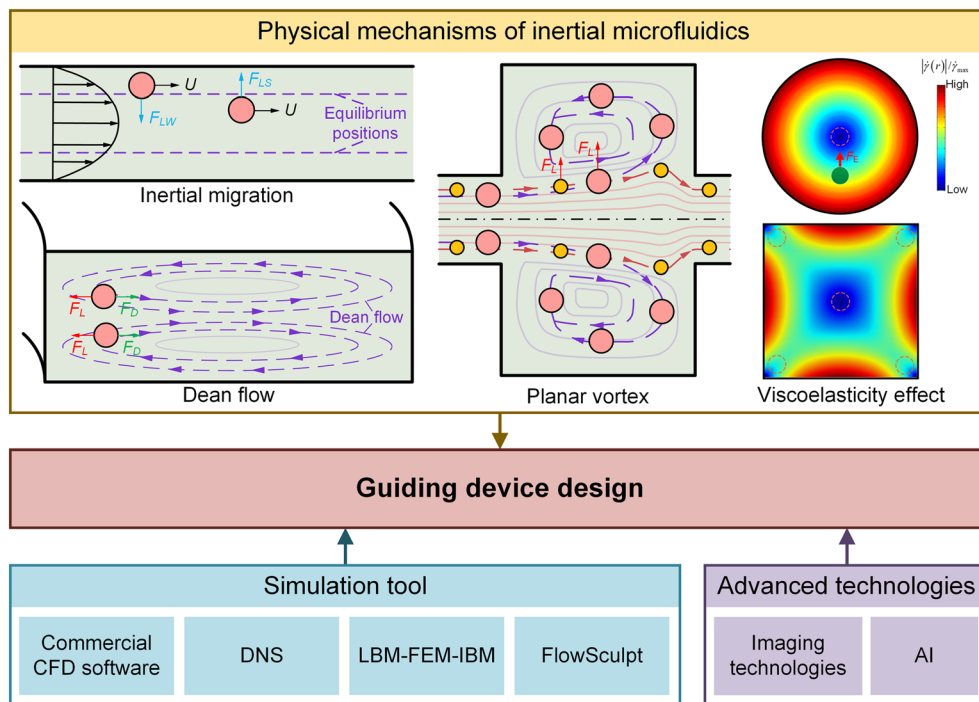


Fig. 1 Physical mechanisms (inertial migration, Dean flow, planar vortex, and viscoelasticity effect), simulation tools (commercial computational fluid dynamics (CFD) software package, direct numerical simulation (DNS), lattice Boltzmann method (LBM)–finite element method (FEM)–immersed boundary method (IBM), and FlowSculpt), and advanced technologies (imaging technologies and artificial intelligence (AI)) for guiding the device design of inertial microfluidics. Images for illustrating the inertial migration, Dean flow, and planar vortex were reprinted from ref. 22 with permission, copyright 2020, The Royal Society of Chemistry. Images for illustrating the viscoelasticity effect were reprinted from ref. 34 with permission, copyright 2019, Springer Nature.

macroscopic flows. Some pioneering studies have noticed this limitation and modified macroscopic equations for microscale conditions;^{40,42} however, most of these modified equations are suitable only for specific conditions. To address this issue, microfluidic researchers should work together with teams specializing in fluid mechanics. Third, the competition between multiple forces remains unclear. An improved understanding of force competition in inertial microfluidics will enable the precise prediction of particle migration. Fourth, the current understanding on particle migration physics is limited to microscale objects. Some studies have successfully used inertial microfluidics for the focusing or separation of sub-microscale particles.^{46,47} With the assistance of viscoelasticity effects, the manipulation of nanoscale materials has been realized.^{48,49} However, the physical mechanisms for manipulating these nanoscale and sub-microscale materials remain unclear. It is noteworthy that many issues in inertial microfluidic physics should be investigated further; herein, we refer to only a few from our perspective.

In addition to design rules, simulations can help researchers quickly design and optimize microfluidic devices.²⁷ Indeed, simulation can help predict the migration trajectories of particles, flow field distributions, and other flow details that are difficult to experimentally observe. Currently, several computational fluid dynamics software packages, including COMSOL and ANSYS, can quickly

simulate the flow and particle distributions in inertial microfluidics. However, most of these commercial software do not consider the finite volume of particles, particle–fluid interactions, and deformation of biological particles. A direct numerical simulation was proposed to calculate the steady-state flow fields around a single particle fixed at a specific cross-sectional position; thus, the inertial lift force acting on the particles can be calculated.⁴² Nonetheless, this method cannot simulate the dynamics of multiple particles in complex channels. Currently, other advanced numerical simulation methods for computational inertial microfluidics are also available. For example, the lattice Boltzmann method is a powerful mesoscopic simulation method for computing fluid–structure interactions and addressing complex boundaries, which when coupled with the finite element method using the immersed boundary method can predict the three-dimensional (3D) migration trajectory of particles, particle–fluid interactions, and particle deformation, thereby facilitating the elucidation of particle focusing mechanisms.^{50,51} These advanced numerical simulation methods play an important role in studying inertial microfluidic physics but are difficult to use by researchers from other disciplines without knowledge of programming and fluid mechanics. As most end users are more focused on the output results rather than on the physical and mathematical aspects of the simulation process, a simulation software with a graphical user interface is more attractive.

Recently, the Di Carlo Lab developed the FlowSculpt software to predict and optimize the interfacial stretching of two coflows^{14,52} and ultimately achieve an optimized design of obstacle sequences for microfluidic mixing,⁹ flow sculpting,¹⁴ and microfiber fabrication.¹³ The development of this ready-to-use software will greatly reduce the time required for designing inertial microfluidics.




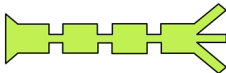
Experimental characterization is still the mainstream approach for studying inertial microfluidic physics and is mainly performed using a microscope and an attached high-speed camera to observe the planar particle distribution in the channels. To obtain the 3D particle trajectory, technologies such as side-view imaging^{53,54} and confocal imaging⁸ have been used to measure the particle distribution in the vertical direction and cross section. However, many advanced measurement technologies in macroscopic fluid mechanics are still rarely used to study inertial microfluidic physics, possibly because of the microscale limit. In the future, the panorama of inertial microfluidic physics can be clearly depicted with the assistance of these advanced measurement and numerical simulation technologies (Fig. 1). Moreover, artificial intelligence may also significantly

contribute to the design of inertial microfluidics. For example, machine learning has been used to assist in the fast prediction of inertial lift in inertial microfluidic channels, which can then be integrated into the Lagrangian tracking method to accurately predict the particle focusing in spiral channels and channels with varied cross-sectional shapes.⁵⁵ In addition, the separation of a desired sample could be quickly regulated using machine learning with failure experiments, which makes it possible to automatically identify the best separation parameters when changing the samples.⁵⁶

Channel innovation for improved performances or new functions

Commonly used channel geometries for inertial microfluidics include spiral, straight, serpentine, and contraction-expansion channels, and their corresponding modified forms, which are appropriate for various applications (Table 1).²² For example, the spiral channel is widely used for particle separation based on differential focusing positions. In spiral channels, differently sized particles will

Table 1 A summary of channel innovations in inertial microfluidics

Channel	Spiral channel	Serpentine channel	Straight channel	Contraction-expansion channel
Geometry				
Dominant forces or hydrodynamic effects	1. Dean drag force 2. Inertial lift force 3. Elastic force (for viscoelastic fluids)	1. Dean drag force 2. Inertial lift force	1. Inertial lift force 2. Elastic force (for viscoelastic fluids)	1. Dean drag force 2. Inertial lift force 3. Planar vortex 4. Elastic force (for viscoelastic fluids)
Functions (★representative function)	1. Separation★ 2. Focusing 3. Concentration 4. Mixing	1. Focusing★ 2. Separation	1. Focusing★ 2. Separation	1. Trapping★ 2. Separation★
Features	1. Continuously varied Dean drag force 2. Easy to miniaturize	1. Periodically varied Dean drag force 2. Easy to parallel	1. Simple geometry 2. Easy to parallel	1. Vortex based trapping 2. Easy to parallel
Channel design parameters	1. Cross-sectional dimension (channel height and width) 2. Initial radius of spiral	1. Cross-sectional dimension (channel height and width) 2. Symmetry and radius of serpentine turns	1. Cross-sectional shape and dimension (channel height and width) 2. Channel length	1. Cross-sectional dimension (channel height and width) 2. Dimensions of contraction and expansion sections
Modified forms	3. Channel length 1. Archimedes spiral 2. Dean flow fractionation (two inlets) 3. Trapezoidal spiral channel 4. Double spiral 5. Spiral with ordered micro-obstacles 6. Labyrinth spiral	3. Channel length 1. Sinusoidal 2. Square-wave 3. Triangular-wave	Straight channels with rectangle, triangle, and half-circle cross-sections	3. Shape of expansion cavity 1. Conventional contraction-expansion channel 2. Channel orthogonally arranged with a series of constrictions in height 3. Channel with sequenced micropillars

simultaneously suffer from the Dean drag force caused by the Dean flow and the inertial lift force induced by the inertial migration effect, thus occupying different focusing positions to facilitate the separation of particles.^{57–59} However, the lateral positions of the focused particle trains are very close in a spiral channel, which makes high-purity separation challenging. To address this issue, Dean flow fractionation (DFF) was developed by coflowing a sample flow with an additional sheath flow.^{60,61} In DFF, the small particles are unfocused and are confined within the original sample flow, whereas the large particles migrate into the sheath flow owing to the strong inertial lift force and Dean drag force. Based on the above principle, the separation accuracy can be greatly increased, but the throughput of the sample flow is relatively low owing to the use of the sheath flow. Nevertheless, this technique was successfully employed for the isolation of sub-microscale circulating extracellular vesicles from blood, which proves the high separation accuracy of DFF.^{47,62} Another optimization approach that has gathered significant attention is the change of cross-section shapes from rectangle to trapezoid,^{54,63,64} which will allow the regulation of the distribution of the cross-sectional Dean flow and consequently the distance between the focused trains of differently sized particles will be increased and the separation accuracy will be enhanced. The trapezoidal spiral channel can separate 10 μm and 12 μm particles with a minimum size difference of 2 μm at a high throughput of 3 mL min^{-1} ,¹² but it is difficult to fabricate using conventional soft lithography. Other modified forms of spiral channels include double spirals,^{65,66} spirals with ordered micro-obstacles,⁶⁷ and labyrinth spirals.⁶⁸ In addition to separation, the spiral channel has been used for enhanced sample mixing,⁶⁹ cell concentration for volume reduction,⁷⁰ and cell focusing for downstream single-cell detection and encapsulation.⁷¹

Serpentine channels, including sinusoidal,^{8,37,38} square-wave,⁷² and triangular-wave⁷³ channels, have been widely used for sheathless particle focusing. In contrast to spiral channels, the Dean drag force varies periodically in serpentine channels, which facilitates sheathless focusing of differently sized particles.³⁷ However, single-line focusing in serpentine channels indeed allows for two focusing positions to exist in the vertical direction (two-dimensional focusing), which overlap from the top view creating the illusion of single-line focusing. In addition to sheathless focusing, the symmetric sinusoidal channel was recently used to achieve cell separation based on the differential focusing statuses (central and two lateral focusing positions) of differently sized particles.^{38,72} However, separation can only be achieved within a narrow operational flow rate range when the focusing statuses of differently sized particles differ. The straight channel is obviously the simplest channel geometry in which the inertial migration effect enables the particles to occupy multiplex focusing positions in the equilibrium cross-section (four positions near the center of each channel side for square cross-sections and two positions near the center of

long channel faces for rectangular cross-sections²⁴). A straight channel is particularly suitable for high-throughput multiplexing parallelization, which was reported to achieve up to 256 high-aspect-ratio channels for image-based extreme-throughput flow cytometry.³⁰ However, multiposition focusing in a straight channel limits its application for separation and downstream detection. To address this limitation, straight channels with nonrectangular cross-sections were developed to reduce the number of focusing positions. Through the connection of channel sections with rectangular, triangular, and half-circular cross-sections, single-position focusing can be successfully achieved at the cost of increasing fabrication complexity.⁷⁴ Another possibility to reduce the number of focusing positions is to couple inertial focusing with viscoelastic focusing (the so-called elastic-inertial focusing), which allows achievement of 3D focusing exactly at the channel centerline without using a nonrectangular cross section.⁷⁵ The contraction–expansion channel can be regarded as a modified geometry of a straight channel. The addition of contraction–expansion array structures induces a cross-sectional Dean flow to differentiate the focusing position for successful separation.⁷⁶ In addition, expansion cavities can induce planar vortexes for trapping particles with diameters larger than a certain threshold.⁷⁷ This working principle has been successfully employed for cell separation,^{11,76–78} vortex-assisted electroporation,⁷⁹ and automatic straining.⁸⁰ Other interesting contraction–expansion channels include channels orthogonally arranged with a series of constrictions in height⁸¹ and channels with sequenced micropillars,⁸² among others.

Although some channel innovations have achieved great success, the optimization and modification of most channels remain aimless. In most previous works, new functions and performance improvements were achieved at the expense of increased fabrication complexity or reduced processing throughput. In the future, novel channels should be developed while considering the actual physical mechanisms of the system. Channels with simple structures and improved performances are urgently needed. Moreover, the manipulation targets of inertial microfluidics are mainly limited to the microscale. The design and optimization of channel structures for the processing of nanometer and millimeter sized particles would be challenging.

Multistage, multiplexing, and multifunction integration for improved performance or diverse applications

Although inertial microfluidics has been successfully used to separate cells based on their differences in shape and deformability, the vast majority of works still realize cell separation based on size difference as the shape and deformability differences of cells are not significant for most samples. The cell separation based on only size difference

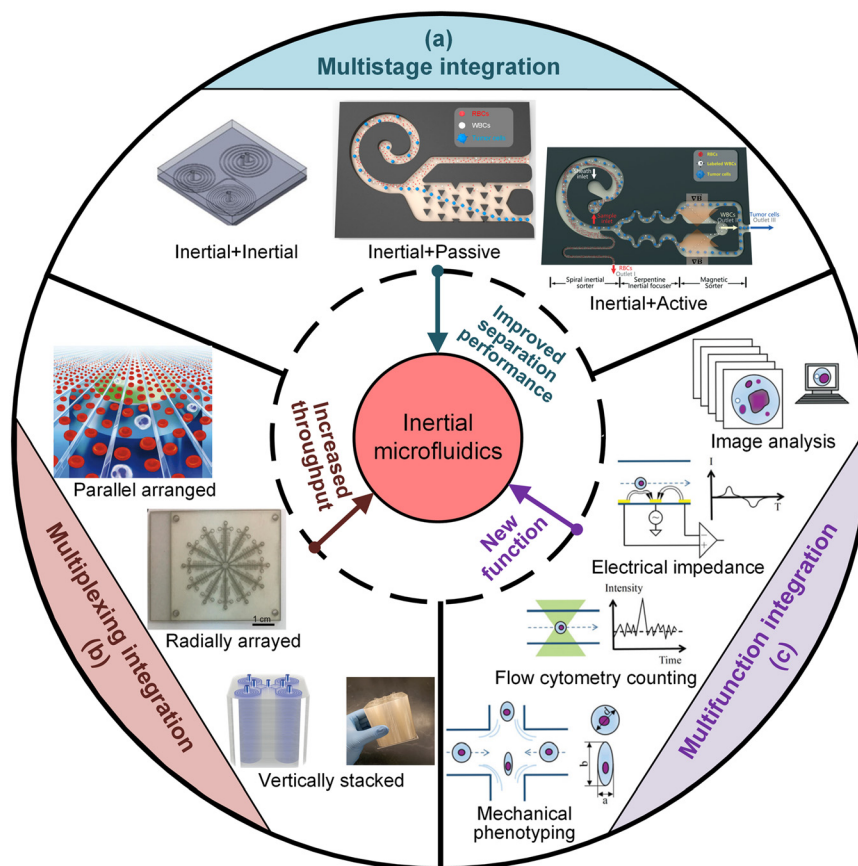


Fig. 2 (a) Multistage (inertial + inertial [reprinted from ref. 83 with permission, copyright 2017, AIP Publishing], inertial + passive [reprinted from ref. 88 with permission, copyright 2019, American Chemical Society], and inertial + active [reprinted from ref. 97 with permission, copyright 2021, The Royal Society of Chemistry]), (b) multiplexing (parallel arranged [reprinted from ref. 30 with permission, copyright 2010, The Royal Society of Chemistry], radially arrayed [reprinted from ref. 101 with permission, copyright 2019, American Chemical Society], and vertically stacked [reprinted from ref. 102 with permission, copyright 2022, The Royal Society of Chemistry]), and (c) multifunction integration (ultrafast optical image analysis, electrical impedance, flow cytometry counting, and mechanical phenotyping) [reprinted from ref. 15 with permission, copyright 2021, The Royal Society of Chemistry] for improved performances (improved separation performance and increased throughput) or new application functions. The representative works and schematic diagram in each category are illustrated.

makes inertial microfluidics unable to separate cells with similar or overlapping sizes, which limits the separation efficiency and purity of the final samples. Multistage integration is a promising approach for addressing this issue (Fig. 2(a)). The most straightforward strategy for multistage integration is serial coupling of the same inertial microfluidic system to improve the purity of the separated samples by repeating the separation process.^{83–86} Another strategy involves the coupling of inertial microfluidics with another passive or active manipulation technique; for example, spiral inertial microfluidics has been integrated with a membrane filter,⁸⁷ deterministic lateral displacement (DLD),^{88,89} and cross-flow filtration.^{90–92} In the case of the two-stage inertial-DLD (i-DLD) sorter, a high sample purity of 93.59% was achieved for the separation of MCF-7 cells from blood cells.⁸⁸ Although DLD has a high separation accuracy, the integrated device cannot eliminate the essence of size-dependent separation and is still unable to separate cells with similar or overlapping sizes. Instead, integration of inertial microfluidics with active cell manipulation methods, which

has attracted increasing interest in recent years, inherits the advantages of both active and passive techniques, possibly to address the size-dependent limitation.^{93,94} For example, inertial microfluidics has been integrated with dielectrophoretic,^{95,96} magnetic,^{97–99} and acoustic¹⁰⁰ methods for cell separation and enrichment. In addition to enhancing the separation performance, dielectrophoresis was used to modify the focusing position and achieve tunable separation in symmetric serpentine channels by the dielectrophoretic force.⁹⁶ Compared with dielectrophoretic and acoustic methods, magnetic separation can be performed without bulk external equipment and is thus easier to miniaturize. In addition, “negative mode” magnetic separation can separate viable circulating tumor cells (CTCs) with low surface protein epithelial cell adhesion molecule expression by magnetically labeling white blood cells (WBCs). Using this negative separation principle, CTC-iChip^{98,99} and i-Mag⁹⁷ devices were successfully developed by combining size-dependent inertial microfluidics with size-independent active magnetophoresis, which were then applied to perform rapid, precise, and

tumor antigen-independent cell separation. High-purity separation is commonly achieved at the expense of decreased cell recovery when multiplex separators are cascaded. Thus, the ideal multistage separation should overcome the size-dependent limitation of inertial microfluidics and comprise the advantages of separators at different stages. We believe that multistage integrated devices with miniaturized footprints and carefully balanced performances will play an important role in various biomedical separation applications.

Inertial microfluidics offers the advantage of high throughput, typically at the mL min^{-1} level, which is much higher than that of most previously reported microfluidic systems.¹⁹ However, this outcome is still not high enough for processing large-volume samples, such as pleural effusions¹⁰³ or bioreaction fluids¹⁰² that can go up to volumes of hundreds of milliliters and hundreds of liters, respectively. To further increase the processing throughput, multiplexing integration of identical inertial microfluidic units (parallel arranged,^{21,30} radially arrayed,^{101,104} and vertically stacked^{102,105–107}) is commonly adopted (Fig. 2(b)). Recently, a multiplexed plastic unit containing 100 vertically stacked spiral channels was developed and successfully applied for ultra-high-throughput clog-free cell filtration at a processing throughput of 1 L min^{-1} , which is attractive for the retention of Chinese hamster ovary cells in the biomanufacturing industry.¹⁰² The major challenge for multiplexing is the integration of as many units as possible in a limited space. Thin polymer-film chips can represent an attractive option for multiplexing integration as it can make full use of the vertical space.^{101,106,107} In addition, the uniform distribution of flow across all branches in a highly integrated device is critical for ensuring the identical performance of each unit, since the performance of inertial microfluidics is highly flow-rate sensitive.

Inertial microfluidics has become an important pretreatment technique for detecting and analyzing unique cell populations (Fig. 2(c)). As a prefocusing unit, the serpentine channel can be integrated with a laser-induced fluorescence system,¹⁷ ultrafast optical image analysis,^{108,109} mechanical phenotyping,^{110,111} and electrical impedance cytometry^{112,113} for high-throughput cell detection. By focusing particles into regular trains, the particles can pass through the interrogation region at a fixed position one by one, thereby avoiding the detection errors caused by the simultaneous existence of multiplex particles in the detection section. In addition, for impedance cytometry and optical imaging, the variation of particle positions also decreases the detection accuracy owing to out-of-focus imaging and attenuation of electrical strength along the vertical direction.¹¹⁴ To deal with rare bioparticles, such as CTCs in peripheral blood that are only 0–50 cells per mL, the efficient isolation and enrichment of these rare cells is a prerequisite for downstream highly sensitive detection. As a highly efficient size-based cell sorter, spiral inertial microfluidics has been widely used for the isolation of CTCs,^{12,58,115,116} sperm cells,^{117,118} exfoliated tumor cells,^{91,119–121} monocytes

with internalized pathogens,¹²² activated lymphocytes,¹²³ circulating fetal trophoblasts,^{124,125} viral particles,¹²⁶ and immune cells¹²⁷ from samples of blood, raw semen, pleural effusion, and sputum with complex background cells. After the enrichment of these target cell populations, the separated cells can be rapidly detected by integrating inertial microfluidics with deep-learning-based cell imaging,¹²⁸ inductively coupled plasma mass spectrometry,^{129,130} single-cell reverse transcription-polymerase chain reaction analysis,¹²⁰ ion mobility mass spectrometry,¹³¹ impedance-based microfluidic assay,¹³² and genetic genotyping.⁷¹ The integration of inertial microfluidic sorting pretreatment significantly reduces the workload of downstream detection and thus increases the detection accuracy. Although great success has been achieved, most multifunction integrations are still performed off-chip, which does not take full advantage of microfluidics features. In the future, we look forward to seeing more interesting applications enabled by integrating inertial microfluidic pretreatment with various novel on-chip detection approaches.

Rapid prototyping for mass manufacturing and creating novel structures

One advantage of inertial microfluidics is its simple channel structure with relatively large dimensions, which makes it especially suitable for low-cost mass manufacturing. However, most previously reported inertial microfluidic devices were fabricated in polydimethylsiloxane using soft lithography,¹³³ which requires a complex fabrication process and a rigorous environment. Compared with channel and application innovations, less attention has been paid to novel rapid prototyping, which facilitates disposable use and low-cost mass manufacturing of inertial microfluidics for various biomedical applications. Recently, several rapid prototyping techniques have been used to design novel nonplanar structures for inertial microfluidics. For example, femtosecond laser irradiation followed by chemical etching has been applied to directly create a 3D serpentine channel in bulk-fused silica glass substrates, which achieved 3D particle focusing at high flow rates (Fig. 3(a)).¹³⁴ However, the fabrication of a long channel using this technique is relatively challenging and time-consuming, as the materials in the channel must be removed by etching. Roll-to-roll (R2R) hot embossing is a large-batch thermoforming process for mass manufacturing microfluidic devices.¹³⁵ An inertial microfluidic device with a simple and low-aspect-ratio straight microchannel was fabricated using R2R hot embossing on polymethyl methacrylate (PMMA) foil and was successfully employed for size-based particle separation (Fig. 3(b)).¹³⁶ However, the channel cross-section fabricated by this process has a trapezoid shape owing to the tooling and demolding processes, which may deteriorate the focusing and separation performances. Another rapid

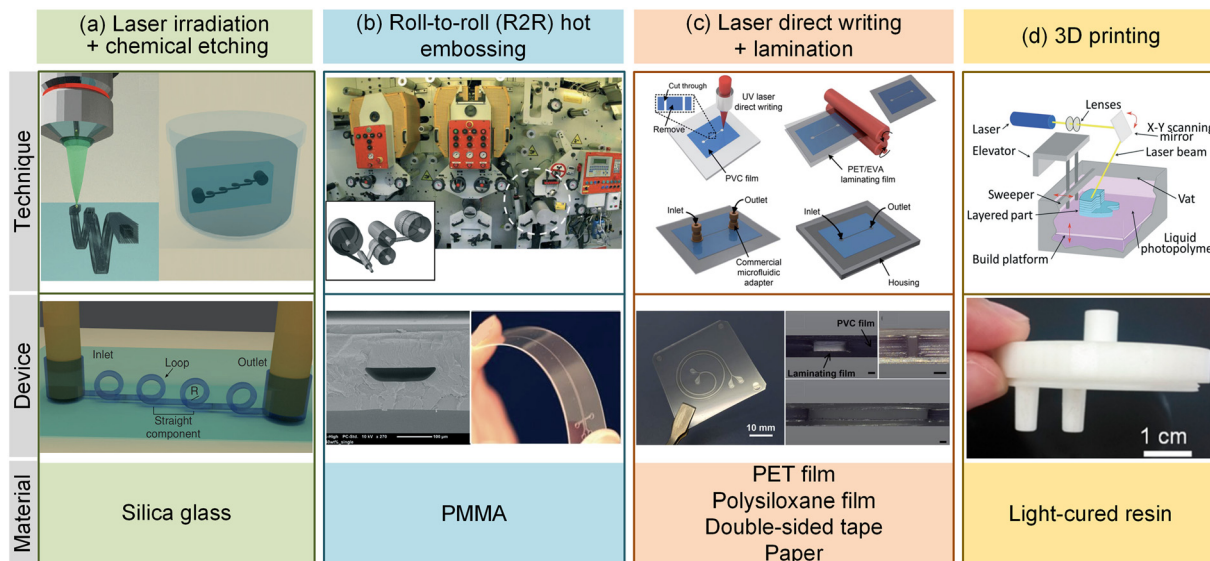


Fig. 3 Rapid prototyping for mass manufacturing and creating novel structures. (a) Laser irradiation + chemical etching [reprinted from ref. 134 with permission, copyright 2017, Springer Nature], (b) roll-to-roll (R2R) hot embossing [reprinted from ref. 136 with permission, copyright 2016, The Royal Society of Chemistry], (c) laser direct writing + lamination [reprinted from ref. 137 with permission, copyright 2016, The Royal Society of Chemistry], and (d) 3D printing [the upper part was reprinted from ref. 139 with permission, copyright 2016, The Royal Society of Chemistry; the lower part was reprinted from ref. 70 with permission, copyright 2018, American Chemical Society]. The representative works showing information on techniques, devices, and materials in each category are illustrated.

prototyping technique used for inertial microfluidics is direct laser writing and lamination, in which the channel patterns are defined by cutting through grooves within the polymer films using a laser-cutting system and the open channel structures are sealed with cover and bottom films *via* lamination (Fig. 3(c)).¹³⁷ This technique can be used to fabricate inertial microfluidic devices with a high speed (<20 min) at an ultralow cost (1.5 cents per chip). Based on this rapid prototyping technique, the multifunctional integration of passive flow regulators with inertial microfluidics for flow-rate-independent operation²⁰ and the integration of multiplexed inertial microfluidic concentrators for processing large-volume samples^{101,106,107} can be successfully achieved. Similar to 3D paper microfluidics,¹³⁸ the adhesion of different or parallel functional layers is realized using double-sided adhesive tape patterned with through-holes; hence, 3D fluidic paths can be constructed in the vertical direction *via* multilayer stacking.¹⁰¹ However, with this method, it is difficult to fabricate channels with dimensions smaller than 20 μm and the channel height is enslaved to the thickness of polymer films.

One newly emerging technique that has gained attraction for fabricating microfluidic devices is 3D printing, which can create 3D structures in bulk materials (Fig. 3(d)).^{139,140} Recently, 3D printing has been successfully applied to build a 3D helical microchannel for size-dependent particle separation.¹⁴¹ However, the dimensions of the printed channels are relatively large; more importantly, it is still challenging to print a long microchannel as the supporting material in a long channel needs to be removed after printing. To ease the removal of the supporting materials,

most inertial microfluidics with long channels are printed on the surface of the material, and then the printed open channel is sealed with a blank plate using double-sided adhesive tape.^{70,142}

In addition to the widely employed polydimethylsiloxane, the device materials polymer film,^{12,101,106,107,137} light-cured resin,^{70,141,142} and PMMA¹³⁶ can be used to fabricate inertial microfluidic devices by various new rapid prototyping techniques, including laser direct writing and 3D printing. Nevertheless, the biocompatibility of most materials used for processing biosamples has not been fully investigated. Recently, a paper-based inertial microfluidics that does not cause environmental pollution was successfully developed at a very low cost.¹⁴³ Unlike traditional paper microfluidics that use capillary force to pump and transfer the sample liquid,¹⁴⁴ paper-based inertial microfluidics can be operated at a high flow-rate throughput and can realize particle enrichment. It is noteworthy that the spiral channel can be constructed to focus and fractionate cells by rolling the “off-the-shelf” microbore tubing.^{144–147} In the future, faster prototyping techniques are warranted to facilitate the development of unconventional inertial microfluidics (with a nonrectangular cross-section and a 3D spatial structure) and mass manufacturing for the commercialization of inertial microfluidics.

Commercial instruments for practical applications

With the improved understanding of device physics and the emergence of new device designs and fabrication techniques, instruments based on inertial microfluidics have been

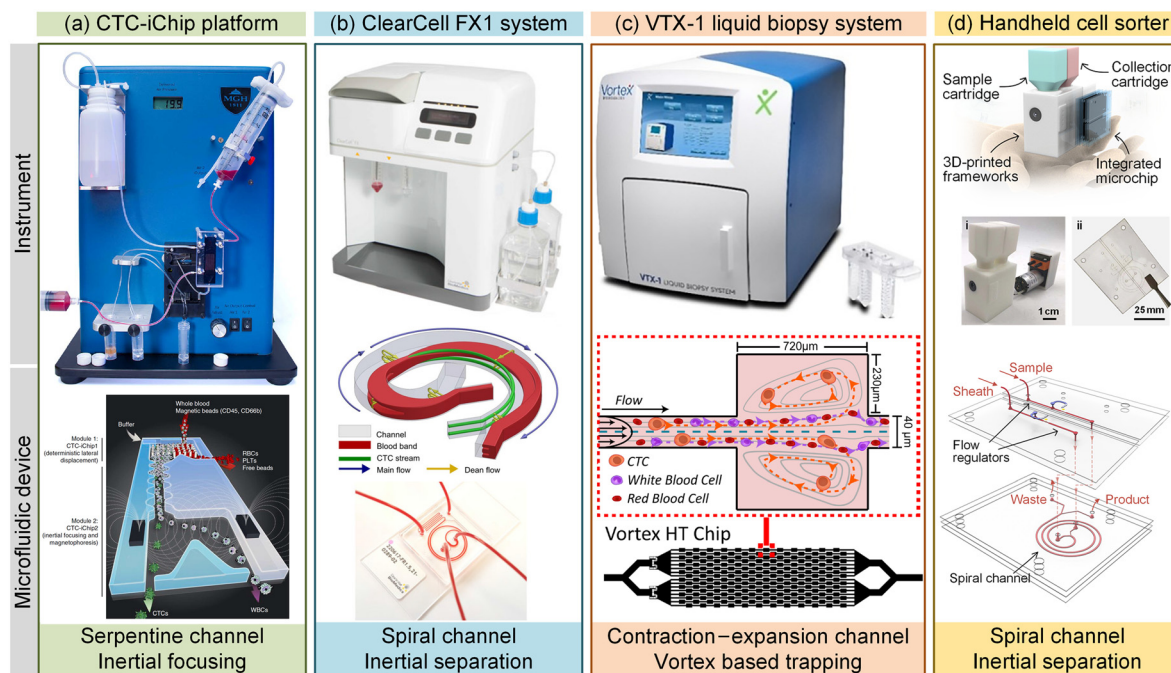


Fig. 4 Commercial instruments based on inertial microfluidics for practical applications. (a) CTC-iChip platform [reprinted from ref. 99 with permission, copyright 2014, Springer Nature], (b) ClearCell FX1 system [reprinted from ref. 148 with permission, copyright 2018, John Wiley and Sons], (c) VTX-1 liquid biopsy system [the upper part was reprinted from ref. 150 with permission, copyright 2018, John Wiley and Sons; the lower part was reprinted from ref. 78 with permission, copyright 2017, Springer Nature], and (d) handheld cell sorter [reprinted from ref. 20 with permission, copyright 2022, American Chemical Society]. Images of instruments and the microfluidic device for each category are illustrated.

successfully developed for biomedical research and disease diagnosis in recent years. In the CTC-iChip platform developed by Toner and colleagues,^{98,99} the serpentine channel-based inertial focusing system was cascaded after the DLD to refocus WBCs, target CTCs, and ensure downstream magnetically activated cell sorting (Fig. 4(a)). In addition to the CTC-iChip platform, the ClearCell FX1 system is a commercially available instrument for label-free isolation of viable CTCs from blood samples (Fig. 4(b)).¹⁴⁸ This system uses a spiral inertial microfluidic channel as the key separation unit to enrich the cell based on the size difference and can be operated in a fully automated manner. Similar to this system, an automated microfluidic cell separation instrument was developed, which contained eight parallel spiral microfluidic channels and nine flow regulators.¹⁴⁹ Its integrated passive flow regulators stabilize the unstable flow generated by the low-cost miniaturized diaphragm pump, thus significantly reducing the footprint and cost of the instrument. Using this microfluidic instrument, tumor cells were separated and concentrated from 5 mL of diluted human blood twice with a high recovery ratio of approximately 85% within a rapid processing time of 23 min. Another successfully commercialized inertial microfluidics is the vortex sorter, which uses the vortices generated in the contraction–expansion structures to trap and enrich large cells.⁷⁸ Based on this principle, a VTX-1 liquid biopsy system was developed for the isolation and purification of CTCs from liquid biopsy samples (Fig. 4(c)).¹⁵⁰ In addition to CTC

isolation, an inertial microfluidic cube integrated with lysis, storage, and extraction modules was developed for the automatic extraction of WBCs from whole blood.¹⁵¹ This system comprises two spiral inertial microfluidic channels designed to achieve complete mixing of whole blood and lysis buffer for red blood cell lysis and extraction of WBCs from lysed blood; an extraction efficiency of 83.9% and a cell viability of 96.6% were achieved. Using a similar extraction principle, an automatic cell-wash platform was developed for cell purification at a throughput of 500 $\mu\text{L min}^{-1}$.¹⁵² In this platform, a serpentine channel with periodic contractions was used to enable the exchange of cells from the original solution to clean the cell washing buffer.

Point-of-care testing approaches can be used for rapid and reliable sample evaluation in nonprofessional environments to aid in disease diagnosis and has attracted increasing interest in recent years.¹⁵³ In addition to these desktop instruments, inertial microfluidics has also been used for the sample preparation of various point-of-care testing. For example, a portable handheld cell sorter integrated with cartridges, shells, and core-integrated microchips was developed for the separation of malignant tumor cells from clinical pleural effusions (Fig. 4(d)).²⁰ In the sorter, a bulky and expensive syringe pump was replaced by a low-cost battery-driven diaphragm pump, and two flow regulators were integrated into the chip to achieve passive regulation of the input flows generated by the low-cost diaphragm pump to drive the spiral inertial microfluidic sorter.

A prominent advantage of inertial microfluidics is that it can be operated by simply driving the flow within a specific flow-rate range. Therefore, the mechanical force provided by the compression spring¹⁵⁴ or the power generated by manually pushing the syringe^{70,155–158} can be used to drive the sample flow in inertial microfluidics, which enables electricity-free operation for use in low-resource settings. We believe that a growing number of inertial microfluidics-based instruments will be developed in the future for widespread biomedical applications.

Conclusion

Based on the provided perspective, herein, we share the current status, challenges, and future opportunities of inertial microfluidics concerning the physical mechanisms, simulation tools, channel innovation, multistage or multifunction integration, rapid prototyping, and commercial device development. First, we discussed the physical mechanisms and simulation tools used to guide the inertial microfluidics device design. Since various nonlinear flow phenomena are involved in inertial microfluidics, particle migration and force competition are very complex and difficult to predict. Thus, an improved understanding of inertial microfluidic physics and the provision of systematic general design rules will address the limitations present in most available devices. Moreover, advanced simulation tools can help researchers to design and optimize devices faster and assist in understanding the physics of inertial microfluidics. Nevertheless, advances should be made to ensure that these software packages can be easily used by professionals across different disciplines. Second, we summarized the most recent advances in channel innovation and multistage, multiplexing, or multifunction integration for improved performance or functionalization. Currently, several channel geometries are available, which allows the use of inertial microfluidics for various applications. In turn, multistage integration can help overcome the size-based separation limitation of most microfluidics systems, which may ultimately impact their applicability in broader research fields. Finally, the development of rapid prototyping techniques for fabricating novel inertial microfluidics and the recent advances in inertial microfluidics-based commercial instruments were discussed. With an improved understanding of the underlying physical mechanisms and the development of novel channels, integration strategies, and commercial instruments, inertial microfluidics with improved performance and outcomes is expected to play an increasingly important role in biomedical research and disease diagnosis.

Conflicts of interest

The authors have no conflicts to disclose.

Acknowledgements

This research work was supported by the National Key Research and Development Program of China (2021YFC2103300), the National Natural Science Foundation of China (51875103 and 81727801), and the Natural Science Foundation of Jiangsu Province (BK20190064).

References

- 1 H. Amini, W. Lee and D. Di Carlo, *Lab Chip*, 2014, **14**, 2739–2761.
- 2 B. Çetin and D. Li, *Electrophoresis*, 2011, **32**, 2410–2427.
- 3 M. Hejazian, W. Li and N.-T. Nguyen, *Lab Chip*, 2015, **15**, 959–970.
- 4 P. Zhang, H. Bachman, A. Ozcelik and T. J. Huang, *Annu. Rev. Anal. Chem.*, 2020, **13**, 17–43.
- 5 P. Paiè, T. Zandrini, R. M. Vázquez, R. Osellame and F. Bragheri, *Micromachines*, 2018, **9**, 200.
- 6 G. Segré and A. Silberberg, *Nature*, 1961, **189**, 209–210.
- 7 W. R. Dean and S. Chapman, *Proc. R. Soc. London, Ser. A*, 1928, **121**, 402–420.
- 8 D. D. Carlo, D. Irimia, R. G. Tompkins and M. Toner, *Proc. Natl. Acad. Sci. U. S. A.*, 2007, **104**, 18892–18897.
- 9 M. Antognoli, D. Stoecklein, C. Galletti, E. Brunazzi and D. Di Carlo, *Lab Chip*, 2021, **21**, 3910–3923.
- 10 J. M. Martel and M. Toner, *Annu. Rev. Biomed. Eng.*, 2014, **16**, 371–396.
- 11 R. Khojah, R. Stoutamore and D. Di Carlo, *Lab Chip*, 2017, **17**, 2542–2549.
- 12 Z. Zhu, D. Wu, S. Li, Y. Han, N. Xiang, C. Wang and Z. Ni, *Anal. Chim. Acta*, 2021, **1143**, 306–314.
- 13 J. K. Nunes, C.-Y. Wu, H. Amini, K. Owsley, D. Di Carlo and H. A. Stone, *Adv. Mater.*, 2014, **26**, 3712–3717.
- 14 D. Stoecklein, M. Davies, J. M. de Rutte, C.-Y. Wu, D. Di Carlo and B. Ganapathysubramanian, *Lab Chip*, 2019, **19**, 3277–3291.
- 15 Z. Zhou, Y. Chen, S. Zhu, L. Liu, Z. Ni and N. Xiang, *Analyst*, 2021, **146**, 6064–6083.
- 16 Y. Chen, Z. Zhou, S. Zhu, Z. Ni and N. Xiang, *Microchem. J.*, 2022, **177**, 107284.
- 17 J. Oakey, R. W. Applegate, E. Arellano, D. D. Carlo, S. W. Graves and M. Toner, *Anal. Chem.*, 2010, **82**, 3862–3867.
- 18 J. M. Martel and M. Toner, *Phys. Fluids*, 2012, **24**, 032001.
- 19 S. Zhu, F. Jiang, Y. Han, N. Xiang and Z. Ni, *Analyst*, 2020, **145**, 7103–7124.
- 20 F. Jiang and N. Xiang, *Anal. Chem.*, 2022, **94**, 1859–1866.
- 21 H. Ren, Z. Zhu, N. Xiang, H. Wang, T. Zheng, H. An, N.-T. Nguyen and J. Zhang, *Sens. Actuators, B*, 2021, **337**, 129758.
- 22 W. Tang, S. Zhu, D. Jiang, L. Zhu, J. Yang and N. Xiang, *Lab Chip*, 2020, **20**, 3485–3502.
- 23 D. Stoecklein and D. Di Carlo, *Anal. Chem.*, 2019, **91**, 296–314.
- 24 D. Di Carlo, *Lab Chip*, 2009, **9**, 3038–3046.
- 25 D. Farajpour, *J. Appl. Comput. Mech.*, 2021, **52**, 168–192.
- 26 A. J. Chung, *BioChip J.*, 2019, **13**, 53–63.

- 27 S. Razavi Bazaz, A. Mashhadian, A. Ehsani, S. C. Saha, T. Krüger and M. Ebrahimi Warkiani, *Lab Chip*, 2020, **20**, 1023–1048.
- 28 D. Huang, J. Man, D. Jiang, J. Zhao and N. Xiang, *Electrophoresis*, 2020, **41**, 2166–2187.
- 29 J. Zhang, S. Yan, D. Yuan, G. Alici, N.-T. Nguyen, M. Ebrahimi Warkiani and W. Li, *Lab Chip*, 2016, **16**, 10–34.
- 30 S. C. Hur, H. T. K. Tse and D. Di Carlo, *Lab Chip*, 2010, **10**, 274–280.
- 31 X. Lu, C. Liu, G. Hu and X. Xuan, *J. Colloid Interface Sci.*, 2017, **500**, 182–201.
- 32 F. Tian, Q. Feng, Q. Chen, C. Liu, T. Li and J. Sun, *Microfluid. Nanofluid.*, 2019, **23**, 68.
- 33 D. Yuan, Q. Zhao, S. Yan, S.-Y. Tang, G. Alici, J. Zhang and W. Li, *Lab Chip*, 2018, **18**, 551–567.
- 34 N. Xiang, Q. Dai, Y. Han and Z. Ni, *Microfluid. Nanofluid.*, 2019, **23**, 16.
- 35 N. Xiang, K. Chen, Q. Dai, D. Jiang, D. Sun and Z. Ni, *Microfluid. Nanofluid.*, 2015, **18**, 29–39.
- 36 J. M. Martel and M. Toner, *Sci. Rep.*, 2013, **3**, 3340.
- 37 D. R. Gossett and D. D. Carlo, *Anal. Chem.*, 2009, **81**, 8459–8465.
- 38 J. Zhang, D. Yuan, Q. Zhao, A. J. T. Teo, S. Yan, C. H. Ooi, W. Li and N.-T. Nguyen, *Anal. Chem.*, 2019, **91**, 4077–4084.
- 39 N. Xiang, H. Yi, K. Chen, D. Sun, D. Jiang, Q. Dai and Z. Ni, *Biomicrofluidics*, 2013, **7**, 044116.
- 40 D. Di Carlo, J. F. Edd, K. J. Humphry, H. A. Stone and M. Toner, *Phys. Rev. Lett.*, 2009, **102**, 094503.
- 41 J. Zhou and I. Papautsky, *Lab Chip*, 2013, **13**, 1121–1132.
- 42 C. Liu, C. Xue, J. Sun and G. Hu, *Lab Chip*, 2016, **16**, 884–892.
- 43 S. Kim and S. J. Lee, *Exp. Fluids*, 2008, **46**, 255.
- 44 N. Nivedita, P. Ligrani and I. Papautsky, *Sci. Rep.*, 2017, **7**, 44072.
- 45 W. Lee, H. Amini, H. A. Stone and D. D. Carlo, *Proc. Natl. Acad. Sci. U. S. A.*, 2010, **107**, 22413–22418.
- 46 L. Wang and D. S. Dandy, *Adv. Sci.*, 2017, **4**, 1700153.
- 47 H. M. Tay, S. Kharel, R. Dalan, Z. J. Chen, K. K. Tan, B. O. Boehm, S. C. J. Loo and H. W. Hou, *NPG Asia Mater.*, 2017, **9**, e434.
- 48 C. Liu, B. Ding, C. Xue, Y. Tian, G. Hu and J. Sun, *Anal. Chem.*, 2016, **88**, 12547–12553.
- 49 C. Liu, J. Guo, F. Tian, N. Yang, F. Yan, Y. Ding, J. Wei, G. Hu, G. Nie and J. Sun, *ACS Nano*, 2017, **11**, 6968–6976.
- 50 D. Jiang, D. Huang, G. Zhao, W. Tang and N. Xiang, *Microfluid. Nanofluid.*, 2018, **23**, 7.
- 51 D. Jiang, W. Tang, N. Xiang and Z. Ni, *RSC Adv.*, 2016, **6**, 57647–57657.
- 52 D. Stoecklein, K. Owsley, C.-Y. Wu, D. Di Carlo and B. Ganapathysubramanian, *Microfluid. Nanofluid.*, 2018, **22**, 74.
- 53 J. Zhou and I. Papautsky, *Biomicrofluidics*, 2021, **15**, 014101.
- 54 G. Guan, L. Wu, A. A. Bhagat, Z. Li, P. C. Y. Chen, S. Chao, C. J. Ong and J. Han, *Sci. Rep.*, 2013, **3**, 1475.
- 55 J. Su, X. Chen, Y. Zhu and G. Hu, *Lab Chip*, 2021, **21**, 2544–2556.
- 56 K. Fukada and M. Seyama, *Anal. Chem.*, 2022, **94**, 7060–7065.
- 57 S. S. Kuntaegowdanahalli, A. A. S. Bhagat, G. Kumar and I. Papautsky, *Lab Chip*, 2009, **9**, 2973–2980.
- 58 M. E. Warkiani, B. L. Khoo, D. S.-W. Tan, A. A. S. Bhagat, W.-T. Lim, Y. S. Yap, S. C. Lee, R. A. Soo, J. Han and C. T. Lim, *Analyst*, 2014, **139**, 3245–3255.
- 59 D. Huang, X. Shi, Y. Qian, W. Tang, L. Liu, N. Xiang and Z. Ni, *Anal. Methods*, 2016, **8**, 5940–5948.
- 60 H. W. Hou, M. E. Warkiani, B. L. Khoo, Z. R. Li, R. A. Soo, D. S.-W. Tan, W.-T. Lim, J. Han, A. A. S. Bhagat and C. T. Lim, *Sci. Rep.*, 2013, **3**, 1259.
- 61 X. Zhang, N. Xiang, W. Tang, D. Huang, X. Wang, H. Yi and Z. Ni, *Lab Chip*, 2015, **15**, 3473–3480.
- 62 H. M. Tay, S. Y. Leong, X. Xu, F. Kong, M. Upadya, R. Dalan, C. Y. Tay, M. Dao, S. Suresh and H. W. Hou, *Lab Chip*, 2021, **21**, 2511–2523.
- 63 M. E. Warkiani, G. Guan, K. B. Luan, W. C. Lee, A. A. S. Bhagat, P. Kant Chaudhuri, D. S.-W. Tan, W. T. Lim, S. C. Lee, P. C. Y. Chen, C. T. Lim and J. Han, *Lab Chip*, 2014, **14**, 128–137.
- 64 L. Wu, G. Guan, H. W. Hou, A. A. S. Bhagat and J. Han, *Anal. Chem.*, 2012, **84**, 9324–9331.
- 65 J. Sun, M. Li, C. Liu, Y. Zhang, D. Liu, W. Liu, G. Hu and X. Jiang, *Lab Chip*, 2012, **12**, 3952–3960.
- 66 J. Sun, C. Liu, M. Li, J. Wang, Y. Xianyu, G. Hu and X. Jiang, *Biomicrofluidics*, 2013, **7**, 011802.
- 67 L. Zhao, M. Gao, Y. Niu, J. Wang and S. Shen, *Sens. Actuators, B*, 2022, **369**, 132284.
- 68 M. Zeinali, M. Lee, A. Nadhan, A. Mathur, C. Hedman, E. Lin, R. Harouaka, M. S. Wicha, L. Zhao, N. Palanisamy, M. Hafner, R. Reddy, G. P. Kalemkerian, B. J. Schneider, K. A. Hassan, N. Ramnath and S. Nagrath, *Cancers*, 2020, **12**, 127.
- 69 A. P. Sudarsan and V. M. Ugaz, *Lab Chip*, 2006, **6**, 74–82.
- 70 N. Xiang, X. Shi, Y. Han, Z. Shi, F. Jiang and Z. Ni, *Anal. Chem.*, 2018, **90**, 9515–9522.
- 71 H.-S. Moon, K. Je, J.-W. Min, D. Park, K.-Y. Han, S.-H. Shin, W.-Y. Park, C. E. Yoo and S.-H. Kim, *Lab Chip*, 2018, **18**, 775–784.
- 72 J. Zhang, S. Yan, R. Sluyter, W. Li, G. Alici and N.-T. Nguyen, *Sci. Rep.*, 2014, **4**, 4527.
- 73 Y. Ying and Y. Lin, *Sci. Rep.*, 2019, **9**, 16575.
- 74 J. Kim, J. Lee, C. Wu, S. Nam, D. Di Carlo and W. Lee, *Lab Chip*, 2016, **16**, 992–1001.
- 75 S. Yang, J. Y. Kim, S. J. Lee, S. S. Lee and J. M. Kim, *Lab Chip*, 2011, **11**, 266–273.
- 76 M. G. Lee, S. Choi and J.-K. Park, *J. Chromatogr. A*, 2011, **1218**, 4138–4143.
- 77 S. C. Hur, A. J. Mach and D. D. Carlo, *Biomicrofluidics*, 2011, **5**, 022206.
- 78 C. Renier, E. Pao, J. Che, H. E. Liu, C. A. Lemaire, M. Matsumoto, M. Triboulet, S. Srivas, S. S. Jeffrey, M. Rettig, R. P. Kulkarni, D. Di Carlo and E. Sollier-Christen, *npj Precis. Oncol.*, 2017, **1**, 15.
- 79 D. A. L. Vickers, M. Ouyang, C. H. Choi and S. C. Hur, *Anal. Chem.*, 2014, **86**, 10099–10105.

- 80 A. J. Mach, J. H. Kim, A. Arshi, S. C. Hur and D. Di Carlo, *Lab Chip*, 2011, **11**, 2827–2834.
- 81 A. J. Chung, D. R. Gossett and D. Di Carlo, *Small*, 2013, **9**, 685–690.
- 82 A. J. Chung, D. Pulido, J. C. Oka, H. Amini, M. Masaeli and D. Di Carlo, *Lab Chip*, 2013, **13**, 2942–2949.
- 83 M. Robinson, H. Marks, T. Hinsdale, K. Maitland and G. Coté, *Biomicrofluidics*, 2017, **11**, 024109.
- 84 B. Miller, M. Jimenez and H. Bridle, *Sci. Rep.*, 2016, **6**, 36386.
- 85 L. Sprenger, S. Dutz, T. Schneider, S. Odenbach and U. O. Häfeli, *Biomicrofluidics*, 2015, **9**, 044110.
- 86 T. H. Kim, H. J. Yoon, P. Stella and S. Nagrath, *Biomicrofluidics*, 2014, **8**, 064117.
- 87 J. Wang, W. Lu, C. Tang, Y. Liu, J. Sun, X. Mu, L. Zhang, B. Dai, X. Li, H. Zhuo and X. Jiang, *Anal. Chem.*, 2015, **87**, 11893–11900.
- 88 N. Xiang, J. Wang, Q. Li, Y. Han, D. Huang and Z. Ni, *Anal. Chem.*, 2019, **91**, 10328–10334.
- 89 H. Pei, L. Li, Y. Wang, R. Sheng, Y. Wang, S. Xie, L. Shui, H. Si and B. Tang, *Anal. Chem.*, 2019, **91**, 11078–11084.
- 90 N. Xiang, Q. Li and Z. Ni, *Anal. Chem.*, 2020, **92**, 6770–6776.
- 91 N. Xiang and Z. Ni, *Lab Chip*, 2022, **22**, 757–767.
- 92 A. Rahi, M. Kazemi, E. Pishbin, S. Karimi and H. Nazarian, *Analyst*, 2021, **146**, 7230–7239.
- 93 H. Cha, H. Fallahi, Y. Dai, D. Yuan, H. An, N.-T. Nguyen and J. Zhang, *Lab Chip*, 2022, **22**, 423–444.
- 94 S. Yan, J. Zhang, D. Yuan and W. Li, *Electrophoresis*, 2017, **38**, 238–249.
- 95 Y. Wang, J. Wang, J. Cheng, Y. Zhang, G. Ding, X. Wang, M. Chen, Y. Kang and X. Pan, *IEEE Sens. J.*, 2020, **20**, 14607–14616.
- 96 J. Zhang, D. Yuan, Q. Zhao, S. Yan, S.-Y. Tang, S. H. Tan, J. Guo, H. Xia, N.-T. Nguyen and W. Li, *Sens. Actuators, B*, 2018, **267**, 14–25.
- 97 D. Huang and N. Xiang, *Lab Chip*, 2021, **21**, 1409–1417.
- 98 A. Mishra, T. D. Dubash, J. F. Edd, M. K. Jewett, S. G. Garre, N. M. Karabacak, D. C. Rabe, B. R. Mutlu, J. R. Walsh, R. Kapur, S. L. Stott, S. Maheswaran, D. A. Haber and M. Toner, *Proc. Natl. Acad. Sci. U. S. A.*, 2020, **117**, 16839–16847.
- 99 N. M. Karabacak, P. S. Spuhler, F. Fachin, E. J. Lim, V. Pai, E. Ozkumur, J. M. Martel, N. Kojic, K. Smith, P.-I. Chen, J. Yang, H. Hwang, B. Morgan, J. Trautwein, T. A. Barber, S. L. Stott, S. Maheswaran, R. Kapur, D. A. Haber and M. Toner, *Nat. Protoc.*, 2014, **9**, 694–710.
- 100 N. Nivedita, N. Garg, A. P. Lee and I. Papautsky, *Analyst*, 2017, **142**, 2558–2569.
- 101 N. Xiang, R. Zhang, Y. Han and Z. Ni, *Anal. Chem.*, 2019, **91**, 5461–5468.
- 102 H. Jeon, T. Kwon, J. Yoon and J. Han, *Lab Chip*, 2022, **22**, 272–285.
- 103 R. Asciak and N. M. Rahman, *Clin. Chest Med.*, 2018, **39**, 181–193.
- 104 A. J. Mach and D. Di Carlo, *Biotechnol. Bioeng.*, 2010, **107**, 302–311.
- 105 M. Rafeie, J. Zhang, M. Asadnia, W. Li and M. E. Warkiani, *Lab Chip*, 2016, **16**, 2791–2802.
- 106 F. Jiang, N. Xiang and Z. Ni, *Electrophoresis*, 2020, **41**, 2136–2143.
- 107 N. Xiang, Q. Li, Z. Shi, C. Zhou, F. Jiang, Y. Han and Z. Ni, *Electrophoresis*, 2020, **41**, 875–882.
- 108 K. Goda, A. Ayazi, D. R. Gossett, J. Sadasivam, C. K. Lonappan, E. Sollier, A. M. Fard, S. C. Hur, J. Adam, C. Murray, C. Wang, N. Brackbill, D. D. Carlo and B. Jalali, *Proc. Natl. Acad. Sci. U. S. A.*, 2012, **109**, 11630–11635.
- 109 A. S. Rane, J. Rutkauskaitė, A. deMello and S. Stavrakis, *Chem*, 2017, **3**, 588–602.
- 110 J. S. Dudani, D. R. Gossett, H. T. K. Tse and D. Di Carlo, *Lab Chip*, 2013, **13**, 3728–3734.
- 111 J. Lin, D. Kim, H. T. Tse, P. Tseng, L. Peng, M. Dhar, S. Karumbayaram and D. Di Carlo, *Microsyst. Nanoeng.*, 2017, **3**, 17013.
- 112 W. Tang, D. Tang, Z. Ni, N. Xiang and H. Yi, *Anal. Chem.*, 2017, **89**, 3154–3161.
- 113 D. Tang, M. Chen, Y. Han, N. Xiang and Z. Ni, *Sens. Actuators, B*, 2021, **336**, 129719.
- 114 H. Daguerre, M. Solsona, J. Cottet, M. Gauthier, P. Renaud and A. Bolopion, *Lab Chip*, 2020, **20**, 3665–3689.
- 115 R. M. Jack, M. M. G. Grafton, D. Rodrigues, M. D. Giraldez, C. Griffith, R. Cieslak, M. Zeinali, C. Kumar Sinha, E. Azizi, M. Wicha, M. Tewari, D. M. Simeone and S. Nagrath, *Adv. Sci.*, 2016, **3**, 1600063.
- 116 A. S. Rzhvskiy, S. Razavi Bazaz, L. Ding, A. Kapitannikova, N. Sayyadi, D. Campbell, B. Walsh, D. Gillatt, M. Ebrahimi Warkiani and A. V. Zvyagin, *Cancers*, 2020, **12**, 81.
- 117 H. Feng, A. Jafek, R. Samuel, J. Hotaling, T. G. Jenkins, K. I. Aston and B. K. Gale, *Analyst*, 2021, **146**, 3368–3377.
- 118 H. Jeon, C. Cremers, D. Le, J. Abell and J. Han, *Sci. Rep.*, 2022, **12**, 4212.
- 119 P.-H. Tsou, P.-H. Chiang, Z.-T. Lin, H.-C. Yang, H.-L. Song and B.-R. Li, *Lab Chip*, 2020, **20**, 4007–4015.
- 120 H. Si, D. Du, W. Li, Q. Li, J. Li, D. Zhao, L. Li and B. Tang, *Anal. Chem.*, 2021, **93**, 10477–10486.
- 121 Z. Zhu, S. Li, D. Wu, H. Ren, C. Ni, C. Wang, N. Xiang and Z. Ni, *Lab Chip*, 2022, **22**, 2097–2106.
- 122 J. Liao, J. Ren, H. Wei, R. H. W. Lam, S. L. Chua and B. L. Khoo, *Biosens. Bioelectron.*, 2021, **191**, 113412.
- 123 C. Petchakup, P. E. Hutchinson, H. M. Tay, S. Y. Leong, K. H. H. Li and H. W. Hou, *Sens. Actuators, B*, 2021, **339**, 129864.
- 124 M. Winter, T. Hardy, M. Rezaei, V. Nguyen, D. Zander-Fox, M. Ebrahimi Warkiani and B. Thierry, *Adv. Mater. Technol.*, 2018, **3**, 1800066.
- 125 Y. Huang, S. Yu, S. Chao, L. Wu, M. Tao, B. Situ, X. Ye, Y. Zhang, S. Luo, W. Chen, X. Jiang, G. Guan and L. Zheng, *Lab Chip*, 2020, **20**, 4342–4348.
- 126 K. Choi, H. Ryu, K. J. Siddle, A. Piantadosi, L. Freimark, D. J. Park, P. Sabeti and J. Han, *Anal. Chem.*, 2018, **90**, 4657–4662.

- 127 H. Ryu, K. Choi, Y. Qu, T. Kwon, J. S. Lee and J. Han, *Anal. Chem.*, 2017, **89**, 5549–5556.
- 128 H. Jeon, M. Wei, X. Huang, J. Yao, W. Han, R. Wang, X. Xu, J. Chen, L. Sun and J. Han, *Anal. Chem.*, 2022, **94**, 6394–6402.
- 129 C. Wu, X. Wei, X. Men, X. Zhang, Y.-L. Yu, Z.-R. Xu, M.-L. Chen and J.-H. Wang, *Anal. Chem.*, 2021, **93**, 8203–8209.
- 130 X. Zhang, X. Wei, X. Men, C.-X. Wu, J.-J. Bai, W.-T. Li, T. Yang, M.-L. Chen and J.-H. Wang, *ACS Appl. Mater. Interfaces*, 2021, **13**, 43668–43675.
- 131 L. Zhang, T. Xu, J. Zhang, S. C. C. Wong, M. Ritchie, H. W. Hou and Y. Wang, *Anal. Chem.*, 2021, **93**, 10462–10468.
- 132 C. Petchakup, H. M. Tay, K. H. H. Li and H. W. Hou, *Lab Chip*, 2019, **19**, 1736–1746.
- 133 Y. Xia and G. M. Whitesides, *Angew. Chem., Int. Ed.*, 1998, **37**, 550–575.
- 134 P. Paiè, F. Bragheri, D. Di Carlo and R. Osellame, *Microsyst. Nanoeng.*, 2017, **3**, 17027.
- 135 S. S. Deshmukh and A. Goswami, *Mater. Manuf. Processes*, 2021, **36**, 501–543.
- 136 X. Wang, C. Liedert, R. Liedert and I. Papautsky, *Lab Chip*, 2016, **16**, 1821–1830.
- 137 X. Zhang, D. Huang, W. Tang, D. Jiang, K. Chen, H. Yi, N. Xiang and Z. Ni, *RSC Adv.*, 2016, **6**, 9734–9742.
- 138 A. W. Martinez, S. T. Phillips and G. M. Whitesides, *Proc. Natl. Acad. Sci. U. S. A.*, 2008, **105**, 19606–19611.
- 139 N. Bhattacharjee, A. Urrios, S. Kang and A. Folch, *Lab Chip*, 2016, **16**, 1720–1742.
- 140 A. V. Nielsen, M. J. Beauchamp, G. P. Nordin and A. T. Woolley, *Annu. Rev. Anal. Chem.*, 2020, **13**, 45–65.
- 141 W. Lee, D. Kwon, W. Choi, G. Y. Jung, A. K. Au, A. Folch and S. Jeon, *Sci. Rep.*, 2015, **5**, 7717.
- 142 S. Razavi Bazaz, O. Rouhi, M. A. Raoufi, F. Ejeian, M. Asadnia, D. Jin and M. Ebrahimi Warkiani, *Sci. Rep.*, 2020, **10**, 5929.
- 143 M. Naseri, G. P. Simon and W. Batchelor, *Anal. Chem.*, 2020, **92**, 7307–7316.
- 144 X. Li, D. R. Ballerini and W. Shen, *Biomechanics*, 2012, **6**, 011301.
- 145 X. Wang, H. Gao, N. Dindic, N. Kaval and I. Papautsky, *Biomechanics*, 2017, **11**, 014107.
- 146 L. Pasitka, D. van Noort, W. Lim, S. Park and C.-F. Mandenius, *Anal. Chem.*, 2018, **90**, 12909–12916.
- 147 X. Wei, X. Zhang, R. Guo, M.-L. Chen, T. Yang, Z.-R. Xu and J.-H. Wang, *Anal. Chem.*, 2019, **91**, 15826–15832.
- 148 Y. Lee, G. Guan and A. A. Bhagat, *Cytometry, Part A*, 2018, **93**, 1251–1254.
- 149 X. Zhang, Z. Zhu, N. Xiang, F. Long and Z. Ni, *Anal. Chem.*, 2018, **90**, 4212–4220.
- 150 E. Sollier-Christen, C. Renier, T. Kaplan, E. Kfir and S. C. Crouse, *Cytometry, Part A*, 2018, **93**, 1240–1245.
- 151 S. Zhu, D. Wu, Y. Han, C. Wang, N. Xiang and Z. Ni, *Lab Chip*, 2020, **20**, 244–252.
- 152 X. Lu and Y. Ai, *Anal. Chem.*, 2022, **94**, 9424–9433.
- 153 S. K. Vashist, P. B. Lippa, L. Y. Yeo, A. Ozcan and J. H. T. Luong, *Trends Biotechnol.*, 2015, **33**, 692–705.
- 154 N. Xiang and Z. Ni, *Talanta*, 2021, **235**, 122807.
- 155 S. Yan, S. H. Tan, Y. Li, S. Tang, A. J. T. Teo, J. Zhang, Q. Zhao, D. Yuan, R. Sluyter, N. T. Nguyen and W. Li, *Microfluid. Nanofluid.*, 2017, **22**, 8.
- 156 N. Xiang, Y. Han, Y. Jia, Z. Shi, H. Yi and Z. Ni, *Lab Chip*, 2019, **19**, 214–222.
- 157 H. Jeon, B. Jundi, K. Choi, H. Ryu, B. D. Levy, G. Lim and J. Han, *Lab Chip*, 2020, **20**, 3612–3624.
- 158 N. Xiang and Z. Ni, *Biosensors*, 2022, **12**, 14.